Archives of Computational Methods in Engineering (2023) 30:4781–4800
https://doi.org/10.1007/s11831-023-09959-0

REVIEW ARTICLE

Artificial Intelligence-Based Approaches for Detection and Classification of Different Classes of Malaria Parasites Using Microscopic Images: A Systematic Review

Barkha Kakkar[1] · Mohit goyal[2] · Prashant Johri[3] · Yogesh Kumar[4]

Received: 19 January 2023 / Accepted: 8 June 2023 / Published online: 23 June 2023

Abstract
Artificial Intelligence has played an essential role in detecting malaria, which aims to reduce the involvement of any human microscopist in order provide an accurate diagnosis with minimum interference from the human being. The main aim of this paper is to create an AI-based system that helps for the detection and classification of malaria parasites in microscopic images. The data has been collected from three different sources to create four classes, i.e., Falciparum, Malariae, Ovale, and Vivax. Later, data pre-processing is done to reduce an image's size and remove the noisy signals. Further, feature extraction techniques are applied to obtain the region of interest by calculating the morphological values, and generating the bounding box around the selected features after applying watershed segmentation. Deep learning models such as DenseNet121, DenseNet201, ResNet152V2, NasNetLarge, MobileNetV2, and the hybridized DenseNet201 and ResNet152V2 are being applied and trained with the dataset. These models have been evaluated using metrics such as precision, loss, F1 score, recall, and accuracy to examine their performance during the training and validation phase. At the time of experimentation, it has been found that MobileNetV2 computed the highest accuracy, and ResNet152V2 has the best loss value by 0.005. Regarding precision, recall, and F1 score, DenseNet121 computed the exact value of 1.00. Besides this, the models are also examined for different classes by computing the actual and predicted values through a confusion matrix.

1 Introduction

Plasmodium parasites are those species of parasites that cause an acute illness called Malaria. It is a life-threatening disease, although people can be prevented and cured. Five species of parasites cause Malaria in human beings, out of which two pose the greatest threat, i.e., plasmodium vivax and plasmodium falciparum [1]. Malaria does not spread to people through contact but is transmitted through the bites of Anopheles mosquitoes. There is a cycle (Fig. 1) that goes like when an Anopheles mosquito bites any malaria-affected person, that insect also gets infected, and when the same mosquito bites another normal person, a parasite, as mentioned earlier, is transmitted into that normal human being's blood which proliferates there [2]. It has also been found that if a pregnant woman gets Malaria, she can transmit that sickness to their unborn offspring. Malaria can also be transmitted via donating organs, transfusing blood, etc. [3].

From one of the studies, it has been found that almost half of the population of the world is on the verge of malaria. In fact, near about 241 million people had malaria in 85 countries, and 627,000 deaths were recorded [4]. Few people are more susceptible to developing severe malaria than others, such as newborns or children under age 5. These women are pregnant, HIV-affected patients, less immune people, etc. [5]. Other vulnerable groups include people entering areas with intense malaria transmission who have not acquired partial immunity from

✉ Barkha Kakkar
barkhavijh@gmail.com

Mohit goyal
mohitims84@gmail.com

Prashant Johri
johri.prashant@gmail.com

Yogesh Kumar
yogesh.arora10744@gmail.com;
yogesh.kumar@sot.pdpu.ac.in

[1] Department of IT, Institute of Technology and Science, Mohan Nagar, Ghaziabad, India

[2] Department of CSE, G.L.Bajaj Institute of Technology and Management, Greater Noida, India

[3] School of Computer Science and Engineering, Galgotias University, Greater Noida, India

[4] Department of CSE, School of Technology, Pandit Deendayal Energy University, Gandhinagar, Gujarat, India

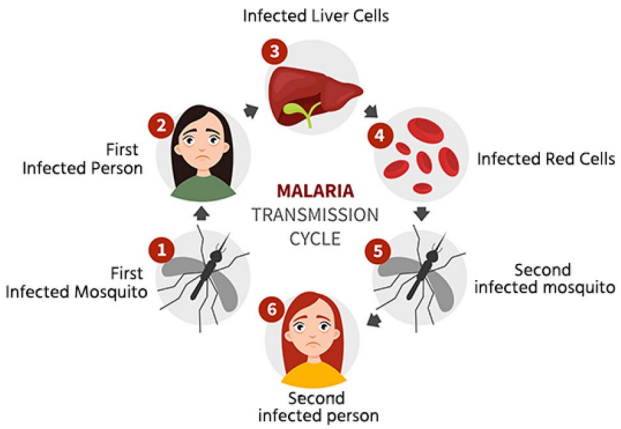

Fig. 1 Life cycle of malaria from an infected to healthy human being [38]

prolonged exposure to the disease or who are not taking chemo-preventive therapies, such as migrants, mobile populations, and travellers [6]. As per the latest report stated by WHO, in 2021, 247 million malaria cases have been reported compared to 2020, which recorded 245 million cases. As far as deaths are concerned, it has risen from 625,000 in 2020 to 619,000 in 2021 [7].

People with partial immunity are at a lower risk of getting affected by malaria than those with low immunity. This is the reason why most of the malaria deaths in Africa occur in young children. WHO states that the African Region carries a disproportionately high share of the global malaria burden [8]. 95% of malaria cases and 96% of malaria deaths in 2021 occurred in the African Region. In the region, 80% of all malaria deaths occurred in children under five. Nigeria (31.3%), the Democratic Republic of the Congo (12.6%), the United Republic of Tanzania (4.1%), and Niger (3.9%) accounted for just over half of all malaria deaths worldwide. Likewise, 1000 natural cases of diseases were reported from 35 countries in 2021, initially from 33 countries in 2020 and 13 countries in 2000 [4]. Countries with zero malaria cases for at least three consecutive years have been eligible for the WHO certification of malaria elimination. Nine malaria-free countries have been certified, such as Maldives in 2015, Sri Lanka and Kyrgyzstan in 2016, Paraguay and Uzbekistan in 2018, Argentina and Algeria in 2019, and China and El Salvador in 2021 [9].

Malaria is diagnosed using various tests such as microscopic examination of blood smears and rapid diagnostic tests to determine whether the parasites are present or not. However, without prompt diagnosis and effective treatment, a case of uncomplicated malaria can progress to a severe form of the disease, which is often fatal without treatment [10]. However, the microscopic examination has become an essential tool to support clinical based research, manage malaria case, and monitor anti-malarial drug efficacy. However, it also takes a lot of time and is completely dependent on the quality level of the blood smear, staining, as well as fixation. Additionally, it has been demonstrated through research that the microscopy-based test misses more than 25% of malaria cases. People who live in inaccessible or difficult-to-reach areas of India experience an increase in these limitations, which is extremely detrimental [11].

This entails developing AI-based etc. microscopic techniques to formulate and use labelled data of malaria parasite images. Various deep learning techniques, such as convolutional neural networks, fully connected networks, U-Nets, encoder-decoder, etc., have been mostly used to segment images, enhance images, and track particles [12]. Deep learning-based models have shown the best performance and have been used widely for analyzing microscopic images based on their speed, flexibility, and low cost. By identifying and classifying drug-induced morphological outliers, AI-based microscopic techniques have primarily been useful to detect drug-resistant parasite strains that have spread throughout Southeast Asia [13]. Due to the AI-powered microscope, malaria parasites can already be observed accurately enough to meet WHO microscopy standards. To avoid the disruption of doctor-patient relationships, gaps in infrastructure of rural India, and in the AI building blocks, the implementation of such a technique necessitates ongoing monitoring and surveillance [14]. For malaria to be eradicated, investments in AI-based microscopy techniques are anticipated to increase diagnostic sensitivity and accuracy in the ensuing decades [15].

In this paper, research has been conducted to develop a deep learning-based model that will detect and classify malaria parasite using microscopic images. The contribution which has been made to accomplish the research is as under:

- Three data repositories have been consulted and are manually combined to create a single dataset consisting of four classes, i.e., Falciparum, Malariae, Ovale, and Vivax.
- In the first step, the microscopic images are initially preprocessed to resize an image's original size and reduce the noisy signals with the help of the Gaussian technique. The images have also been converted to Grayscale images for further computation.
- In the second step, morphological values of images for different parameters, such as area, perimeters, mean color intensity, etc., are calculated. Further, histogram equalization techniques, thresholding, image inverting, image opening, and segmenting the image through the watershed technique are applied to highlight and plot the affecting area. Afterward, the image set is split into training and validation sets by 70:30.
- Further, the images are being trained on various deep learning models such as DenseNet121, DenseNet201, MobileNetV2, ResNet152V2, NASNetLarge, and hybridized model of DenseNet201 and ResNet152V2.

- Ultimately, these applied deep learning models are being evaluated using various parameters such as accuracy, F1 score, loss, recall, and precision. Besides this, the confusion matrix has also been generated to examine the performance of models for different classes.

1.1 Format of the Paper

The format of the paper goes like this; Sect. 1 is the introductory part which has already been covered above it. Section 2 briefly describes the various literature work to identify and classify malaria parasites from microscopic images using multiple machine and deep learning models. Section 3 explains the methodology used to conduct the research, including information regarding the dataset, pre-processing, feature extraction, models that have been applied, and parameters to evaluate their performances. Section 4 demonstrates the results of the models, followed by the discussion part in Sect. 5. The final section, i.e., Sect. 6, summarizes the paper with the challenges faced and the future scope.

2 Related Work

In this section, the work done by researchers in the field of detecting and classifying malaria parasites is shown. In paper [16], the researchers worked on 27,558 cell images which were divided into two classes, i.e., parasitized (contains Plasmodium) and uninfected (no Plasmodium) cells, and trained them on various machine and deep learning techniques. The researchers resampled the images' sizes and applied consistent color to them. Later, a fast convolutional neural network and support vector machine was used to classify the images, which were also compared with the performances of the existing techniques. During experimentation, it was found that the proposed algorithm computed the highest accuracy by 96.7% and 99.4 area under curve value. Likewise, the researchers in their paper [17] proposed a robust CNN model that automatically predicts and classifies infected cells in thin blood smears using standard microscopic slides. The researchers worked on 27,558 single-cell images and used tenfold cross-validation to understand the parameter of the cell. The researchers in the paper [18] used a Visual Geometry Group and Support vector machine to identify the infected falciparum malaria parasite. In the initial stage, K layers of the VGG model were fetched, and SVM was used to replace n-k layers. The researchers created digital malaria set with blood smear images of infected and uninfected malaria patients to evaluate the VGG-SVM model. During implementation, the suggested method approach successfully identified 93.1% of cases of infected falciparum malaria. In their paper [19], the researchers developed ensemble learning models consisting of VGG16 and VGG19, and DenseNet201 for identifying malaria parasites in red blood cells. Various image processing techniques, including the data augmentation technique, were applied to increase the data and solve the overfitting modeling error. While experimenting, it was found that the proposed ensemble learning model obtained a 97.92% model for classifying parasitized and uninfected cells. The researchers in the paper [20] discussed the development of a model for the detection of malaria based on medical data captured from the record of malaria patients in Father Muller Medical college hospital from 2014 to 2018. The researchers studied three algorithms, i.e., XGB classifier, random forest classifier, and gradient boost, where they found that random forest obtained the highest accuracy by 90.97%. The researchers in the paper [21] improved malaria diagnosis using a convolution neural network on the patches that had been segmented from microscopic images of red blood smears. The automatic parasite detection models were designed using three pre-trained models such as VGG19, Resnet50, and MobileNetV2. They were trained with the data taken from Giemsa stained smears collected from the National Institute of Health malaria dataset. It was found that the model obtained 100% accuracy in evaluating these models. The researchers in the paper [22] worked on the efficiency of a deep learning model to detect the deadly disease, i.e., malaria. The researchers applied a convolutional neural network on real-time data to detect malaria effectively and accurately from input images and reduced manual labor by developing a mobile application. The performance of the CNN model was also evaluated using cyclical stochastic gradient descent (SGD) optimizer, where it obtained an accuracy of 97.30% and classified the healthy and infected cell images. As per the researchers, the outcome of their paper would aid in diagnosing malaria, provide reliability to the treatment, and solve the lack of medical expertise. In the paper [23], the researchers worked on developing a deep-learning model that automatically identified malaria-infected cells. The researchers used whole slide images of thin blood stains for compiling malaria-infected red blood cells with the non-infected cells. Three deep learning models were evaluated, which include LeNet, AlexNet, and Google Net, and they obtained an accuracy of 95%. The researchers in the paper [24] explored the advancement in the detection of microscopic malaria detection. The researchers stated that deep learning has been the faster and more efficient extraction of features, examined various deep learning models, and evaluated them on the performance of their accuracy and faster resolution, where it had been found that the ResNet50 model achieved the highest accuracy of 97.55%. In paper [25], the researchers identified whether the malaria parasite exists in the thick of blood smear images using a computer-aided

diagnosis tool. The images for the research were taken from Makerere University AI Research Group. The tool was evaluated using performance metrics such as K fold cross validation, RMSE, and AUC and computed with 75% accuracy. The researchers in paper [26] worked on 27,558 images collected from the Kaggle dataset and resized those 300 × 300 pixels. The researchers applied the Naïve Bayes classifier to detect malaria disease and computed an accuracy of 84%. The researchers in [27] did pre-process, segmentation, extracting of features, and classified the models for the detection and classification of malaria cells in blood smear images. The segmentation was performed using the fuzzy C means method and active contour model. At the same time, the features were extracted by statistical and local directional patterns and later fed into the suggested Chronological Sine Cosine Algorithm (SCA) based Deep CNN classifier. The accuracy obtained was 98.7%. In the paper [28], the researchers applied machine learning models such as Residual CNN, K nearest Neighbour, and Support Vector Machine on 27,558 images of malaria cells collected from the National Institute of Health. The accuracy obtained was 99.90%. The researchers in the paper [29] created a model that combined the advantage of deep learning models such as MobileNet224 with machine learning techniques such as Logistic Regression to extract the features automatically to enhance performance and improve its accuracy. The work was conducted on 9760 images, and the accuracy obtained was 97.03%.

Moreover, the aforementioned work of the researchers has also been analyzed to determine the best model for identifying and classifying malaria parasites in microscopic images. From Fig. 2, while examining the accuracy of machine learning models, it has been found that the XGB classifier obtained the highest accuracy, with 90.97%. Likewise, comparing the deep learning models, the best performance has been obtained by ensemble deep learning models by 97.92%. But when the machine and deep learning models are combined for the same cause, the highest accuracy has been achieved by recurrent neural network and support vector machine with 99.9%, which is, in fact, the highest among all the mentioned accuracy of the techniques used by the researchers.

3 Materials and Methods

This section shows the framework (Fig. 3) used to develop a model that can identify and classify malaria parasites in microscopic images using deep learning models. The work has been conducted using the python language. Various libraries, such as Numpy, Pandas, Matplotlib, seaborn, Opencv, Keras, TensorFlow, etc., have been used to execute the models and functions being used for various purposes [42].

3.1 Dataset

The data for identifying the malaria species in microscopic images have been taken from three sources. All these images have been combined manually to train multiple deep-learning models as shown in Fig. 4. In one of the datasets, there are images of fives species of Plasmodium class that spread malaria in humans: Falciparum, Ovale, Malariae, Vivax, and Knowlesi. The two most prevalent species are P. vivax and P. falciparum. The most dangerous strain, P. falciparum, causes the majority of malaria-related deaths worldwide. Plasmodium knowlesi is also a rare parasite [30]. Another dataset contains 1364 images (~ 80,000 cells) images of Vivax species. Each image has a separate description of each cell in the image, stored in [.json] format [31]. The third form of a

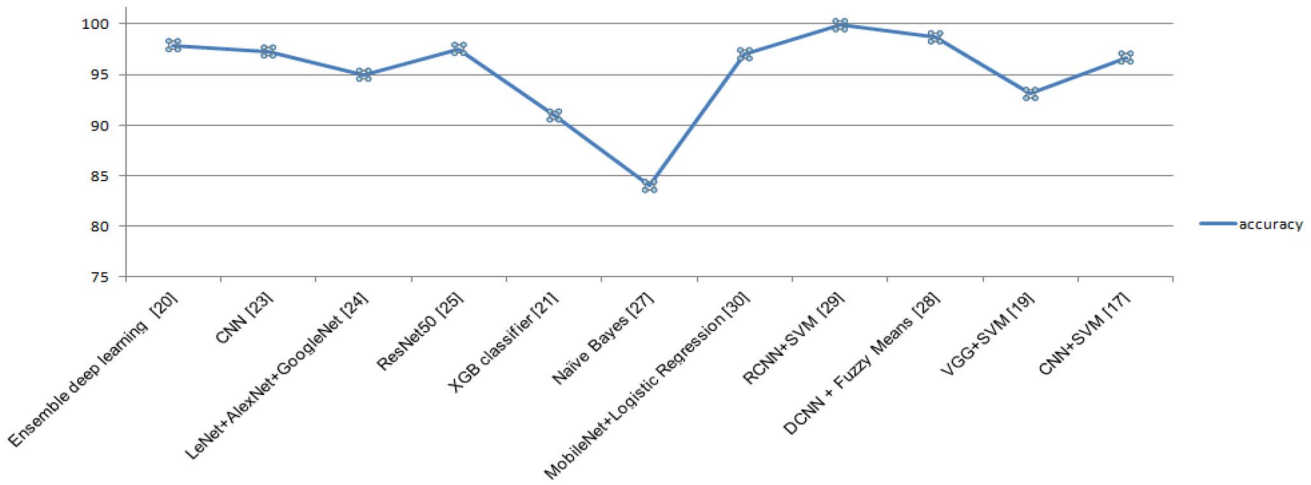

Fig. 2 Analysis of existing models on the basis of their accuracies to detect malaria parasite

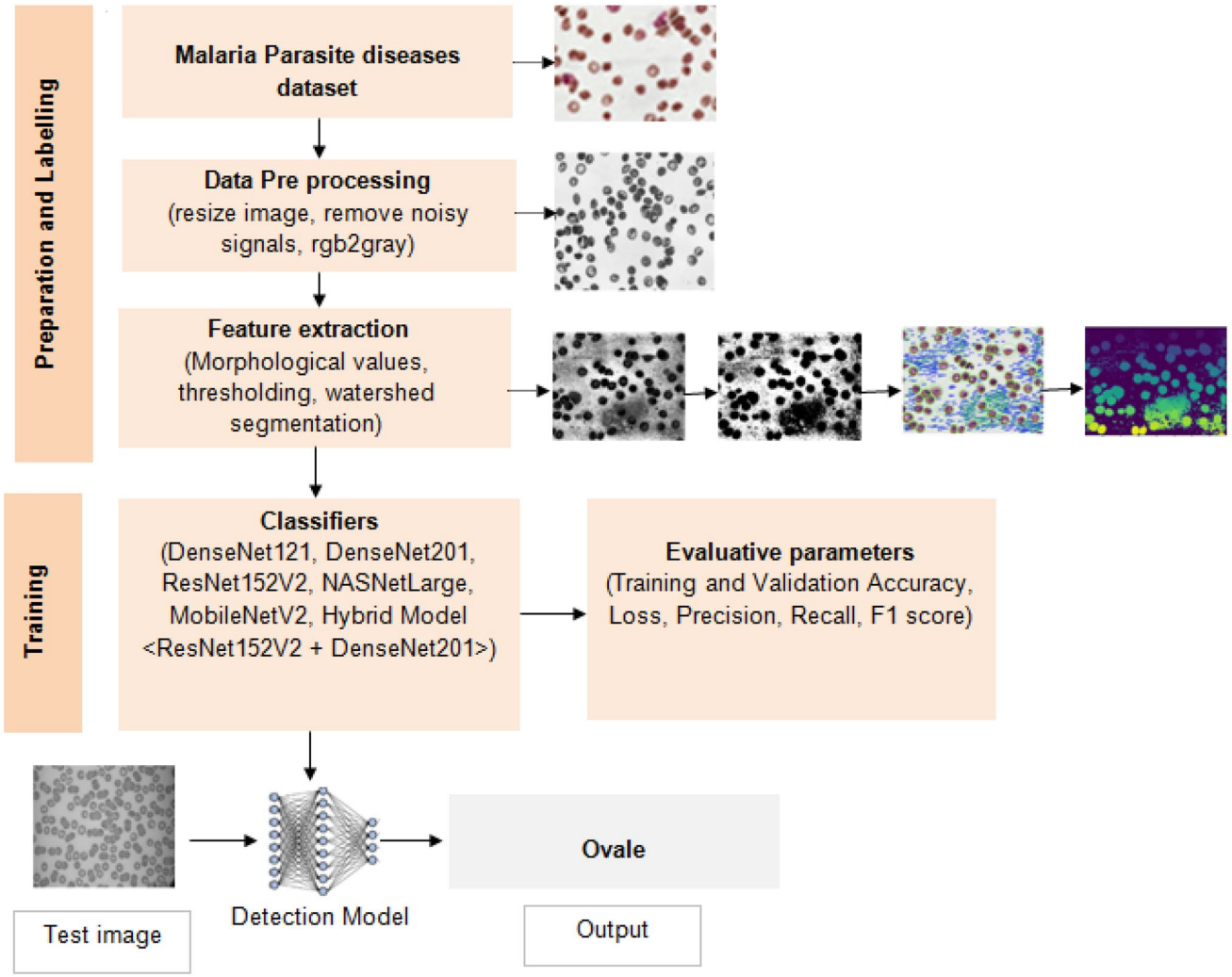

Fig. 3 Proposed system design for the detection and classification of malaria

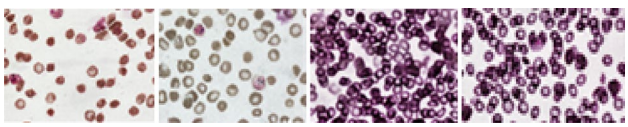

Fig. 4 Sample of microscopic images of malaria parasite

dataset contains 1182 images of thick smears of Falciparum species. Each image has a separate description of each cell in the image, stored in [XML] format. The XML file contains a detail description of the bounding box of each cell which contains falciparum species [32].

3.2 Pre-processing

Data pre-processing is the first step in developing any detection and classification model. During pre-processing of the images, we enhance its quality. Initially, the size of the images was reduced to 64×64 pixels so that we do not have to feed a large number of unnecessary features to the neural network model. Afterwards, the Gaussian blur technique was applied for the removal of noisy signals and all images are converted to grayscale for the simplification of an algorithm by reducing its requirements for computation as shown in Fig. 5.

3.3 Feature Extraction

The data are in the form of images, so we do not have comma-separated values. Hence, we have computed some additional values that will be useful during feature extraction, giving us morphological information about images as shown in Table 1. To determine the area of an image, we need to multiply its height and width in pixels. After calculating the area, we can then find the aspect ratio by dividing

the width of the image by its height. The equations to compute them are (1) and (2)

$$area = height * width \tag{1}$$

$$Aspect\ Ratio = \frac{width}{height} \tag{2}$$

Further, as shown in eq(iii and iv), the height and width of an image can be determined by passing the contour feature points to the bounding rectangle() function in the OpenCV library. These parameters are computed based on the contour feature points and can vary depending on the specific image being analyzed.

$$height = cv2.boundingRect(cnt) \tag{3}$$

$$width = cv2.boundingRect(cnt) \tag{4}$$

Additionally, perimeter, extent, equivalent diameter, and epsilon are determined using Eqs. (5–8). The perimeter is calculated by measuring the arclength of the object's boundary, while the extent is determined by dividing the object's area by the area of its bounding rectangle. The equivalent diameter is comparable to the contour area of the image. Finally, epsilon is computed to find the distance between two points in the same class.

$$epsilon = \sqrt{(x_2 - x_1)^2 + (y_2 - y_1)^2} \tag{5}$$

$$Perimeter = 0.1 * cv2 * arclength(cnt, True) \tag{6}$$

$$Extent = \frac{object\ area}{bounding\ rectangle\ area} \tag{7}$$

$$Equivalent\ diameter = \sqrt{\frac{4 * contourarea}{\pi}} \tag{8}$$

Furthermore, the minimum and maximum value locations of the feature are identified, as well as the minimum and maximum values themselves, by using Eq. (9–12). Additionally, the color intensity value which refers to the brightness or darkness of a particular color in an image is also calculated as a part of this process.

$$Minimum\ value\ Location = cv2.\text{minMaxLo}() \tag{9}$$

$$Maximum\ value\ Location = cv2.\text{minMaxLo}() \tag{10}$$

$$Minimum\ value = cv2.\min() \tag{11}$$

$$Maximum\ value = cv2.\max() \tag{12}$$

$$Mean\ Color = cv2.\text{mean}() \tag{13}$$

Finally, the extreme values of the leftmost, rightmost, bottommost, and topmost points are computed. In this calculation, a value of 0 for the extreme right and leftmost points indicates that the calculation is being done in the horizontal direction, while a calculation in the vertical direction is denoted by a value of 0 for the extreme bottommost and topmost points.

Table 1 Morphological values of microscopic images of malaria parasite

Perimeter	Falciparum	Malariae	Ovale	Vivax
Area	3.0	124.0	1.0	2.0
Perimeter	4.0	45.45	2.0	4.0
Epsilon	0.4	4.54	0.2	0.4
Width	3	15	1	2
Height	1	13	1	1
Aspectratio	3.0	1.15	1.0	2.0
Extent	0.0	0.63	0.0	0.0
Equivalentdiameter	0.0	12.56	0.0	0.0
Minvalue	129.0	49.0	128.0	131.0
Maxvalue	132.0	147.0	128.0	135.0
Minvaluelocation	245,749	58,80	2203,1943	254,1199
Maxvaluelocation	243,749	62,73	2203,1943	253,1199
Meancolor	131.0	107.95	128.0	133.0
ExtremeLeftmostpoint	243,749	50,83	2203,1943	253,1199
Extremerightmostpoint	245,749	64,75	2203,1943	253,1199
Extremetopmostpoint	243,749	58,73	2203,1943	253,1199
Extremebottommostpoint	243,749	59,85	2203,1943	253,1199

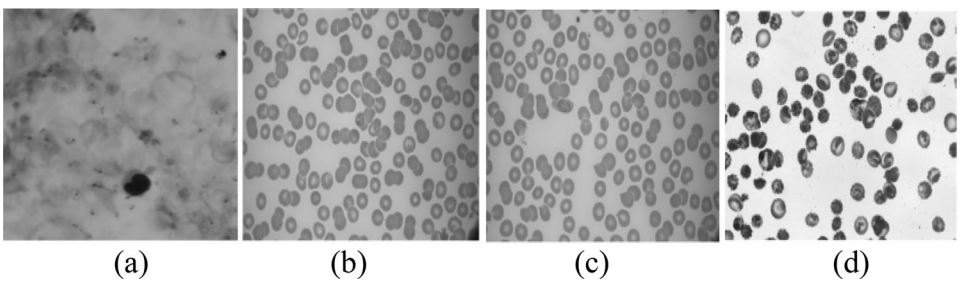

Fig. 5 Pre-processed images **a** Falciparum **b** Malariae **c** Ovale **d** Vivax

$$\textit{Extreme Leftmost point} = \textit{tuple}(\textit{cnt}(\textit{cnt}[:,:,0].\textit{argmin}()[0]) \tag{14}$$

$$\textit{Extreme Rightmost point} = \textit{tuple}(\textit{cnt}(\textit{cnt}[:,:,0].\textit{argmin}()[0]) \tag{15}$$

$$\textit{Extreme Topmost point} = \textit{tuple}(\textit{cnt}(\textit{cnt}[:,:,1].\textit{argmin}()[0]) \tag{16}$$

$$\textit{Extreme Bottommost point} = \textit{tuple}(\textit{cnt}(\textit{cnt}[:,:,1].\textit{argmin}()[0]) \tag{17}$$

Besides calculating morphological values, we have used cv2.equalizehist() to equalize the pixels of an image. For histogram equalization, we have taken grayscale images generated during pre-processing (as shown in Fig. 5). The histogram equalization technique is applied to enhance the contrast of an image so that all the features will be visible to us. Further, thresholding is applied to distinguish between the background and the foreground. We have used cv2.threshold() to calculate the threshold value followed by cv2.bitwise_not(), which performs bitwise not operation on pixels individually for inverting the image. In this phase, the pixels of the highlighted portion or area become 0, and the rest of the pixels become non-zero. Image inversion involves converting the intensity values of an image to their opposite value. For example, white pixels become black and vice versa. Image inversion is useful for enhancing certain features in the image that may be difficult to distinguish with a normal image. For instance, if an object is darker than its background, inverting the image can make it easier to see the edges of the object.

Later image opening which is a morphological operation is applied by using cv2.morphologyEx(). It is used to remove small objects and smooth out the edges of larger objects in an image. It involves the combination of two other morphological operations: erosion and dilation. Erosion removes small objects and thin structures from an image, while dilation smoothes out the edges of the remaining objects. Image opening is useful for removing noise from an image and reducing the complexity of the image, making it easier to extract important features. Here, the boundary pixels which have been removed are grouped with the closest feature that segments the particular area from the rest of the part.

In feature extraction, both image inversion and opening can be used to enhance certain features of an image. For example, in object detection tasks, image inversion can be used to improve the contrast between the object and its background, making it easier to identify the object. Image opening can be used to remove noise and small objects from the image, which can help to simplify the image and make it easier to identify larger objects.

Further, the region-based Watershed segmentation technique is applied using cv2.watershed(). This technique separates image objects based on their edges and intensity values using the image morphology generated in the previous step. As shown in Fig. 6, the affected areas are then highlighted and plotted in various colours. After feature extraction, the essential step is to divide the images into two sets, training and validation, in the proportion of 70:30.

3.4 Applied Models

After obtaining the region of interest, these images have been trained on various models such as DenseNet201, NasNetLarge, MobileNetV2, ResNet152V2, and Densenet121. These models have been evaluated using different parameters, as shown in sec 3.5, to examine their performance. Along with these, two models have been hybridized, i.e., ResNet152V2 and Densenet121, and trained with the same dataset to evaluate the same parameter metrics. In addition to this, the optimizer used in this case is Adam, which is a popular optimization algorithm used in deep learning. The learning rate used during the training is set to 0.02, which determines the magnitude of updates to the model weights during training. The kernel size used in the convolutional layers of the model is set to 3×3, which determines the size of the window that slides over the image during convolution. The activation function used in the output layer of the model is Softmax, which is commonly used for multi-class classification tasks to convert the model's output to a probability distribution over the classes. The input images used during the training have a size of 64×64 pixels, which means that the images have 64 pixels in both the width and height dimensions. Finally, the batch size used during training is set to 64, which determines the number of samples that are processed at once during training but it is not fixed. A larger batch size can result in faster training times, but it may also lead to less accurate weight updates, while a smaller batch size may lead to more accurate weight updates, but slower training times.

3.4.1 DenseNet 201

In the DenseNet201 model, there are 201 layers in which the input layer generates the output shape of (None,64,64,3), which means the batch size is not fixed, height is 64, width is 64, and the number of channels is 3 with zero parameters. Later conv2d layer is added, generating the same output pattern with 84 parameters. The global average pooling2d is added, generating the output in the form of (None, 1920) and zero parameters. Likewise, the

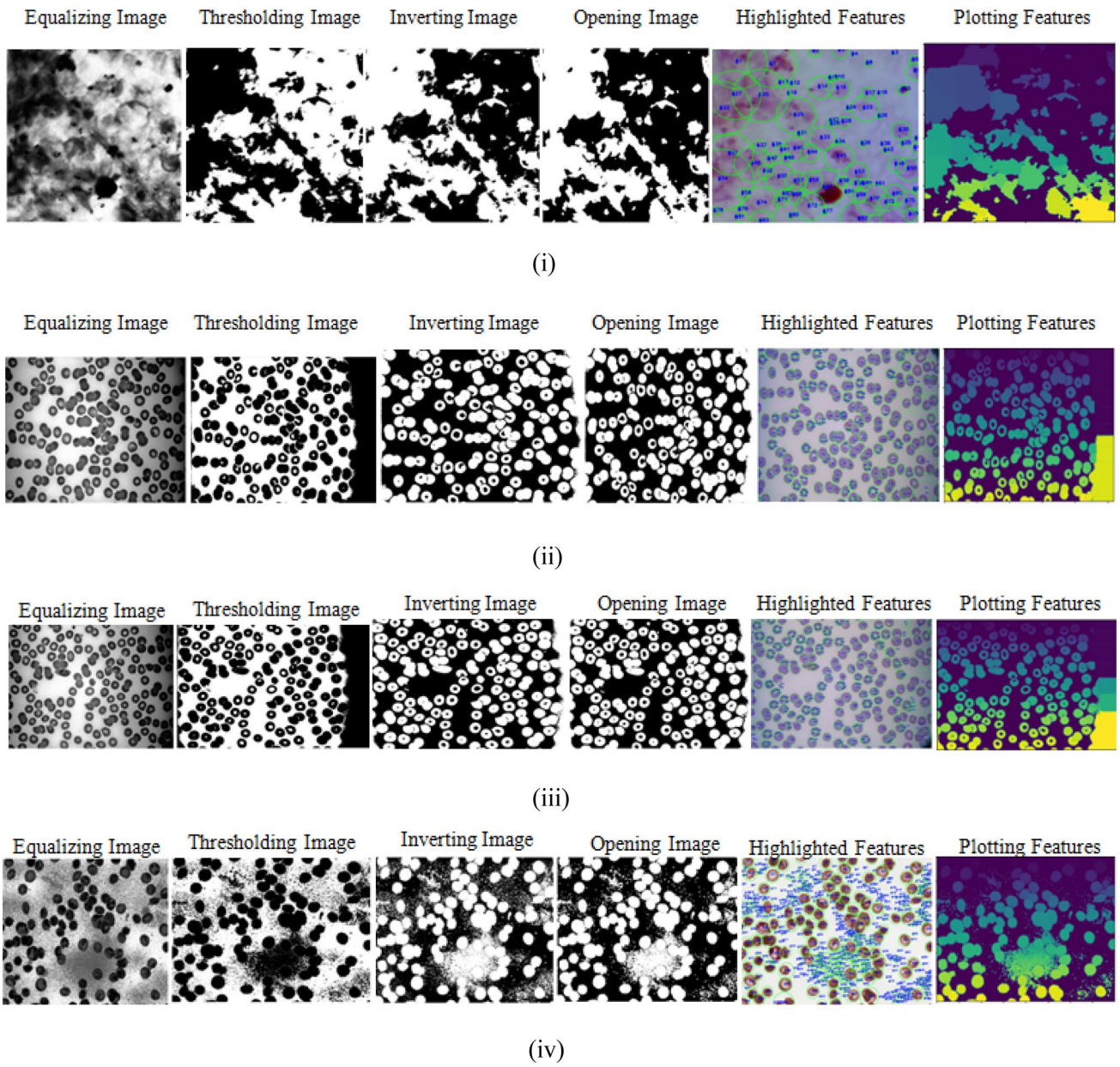

Fig. 6 Feature extraction of microscopic malaria parasite image **i** Falciparum **ii** Malariae **iii** Ovale **iv** Vivax

other layers, such as batch normalization, are added, which trained 7680 parameters, followed by the dropout layer. After the dropout layer, we have a dense layer, one more batch normalization layer, and a dropout and dense layer. The first dense layer train 491,776 parameters, and the last dense layer train 1028 parameters by having the output shape of (None,4). The multiple output layers generated by the DensenNet201 model have 18,321,984 parameters. The total parameters trained by the model are 18,823,576, out of which the trainable parameters are 18,590,168 and the non-trainable parameters are 233,408. The architecture of the DenseNet201 model is shown in Fig. 7.

3.4.2 NASNetLarge

NasNetlarge stands for neural search architecture network. In this architecture, we have normal and reduction cells that return the value of the feature map. For this research, we have used NASNetLarge with the layered architecture of the input layer with (None, 64, 64, 3) output shape and zero parameters. This layer is added to the conv2d layer, which generates the same output with dynamic batch size, 64×64 height and width, and three channels, including 84 parameters that have been trained. The NASNet model generates the multiple output shapes and trained 84,916,818 parameters

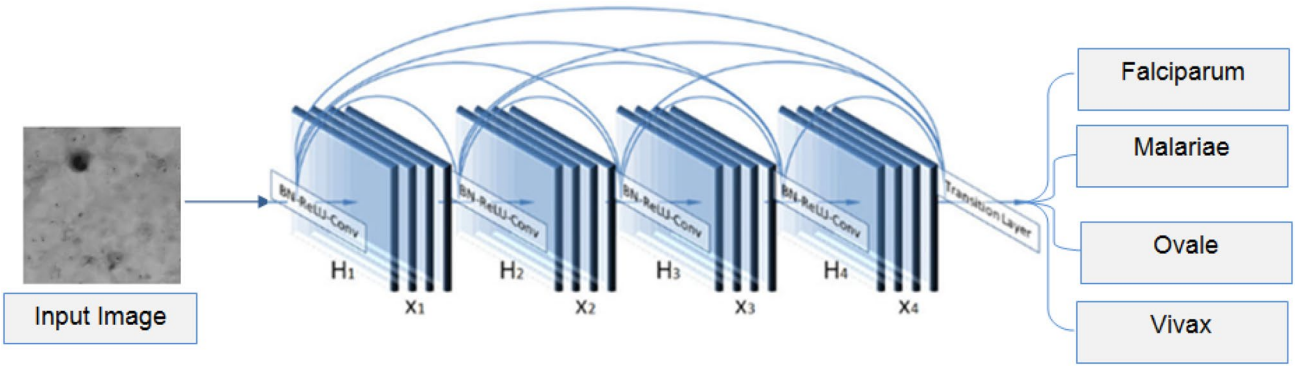

Fig. 7 Architecture of DenseNet201

on those layers. The layer is added to the global_average_pooling2d layer, which generates the output shape of (none,4032) and trains zero parameters. This layer is further linked with the batch normalization layer with the output shape (none, 4032), and each layer trained 16,128 parameters. This particular layer is added to the dropout and dense layer with 4032 and 256 units, respectively, and 1,032,448 parameters were trained. In the end, batch normalization, dropout, and dense layer were added, which generated 256 units which were added to generate the 1024,0, and 1028 parameters, respectively. The total parameters generated were 85,967,530, out of which trainable are 85,762,286 and non-trainable are 205,244. The architecture of the NASNet-large model is shown in Fig. 8.

3.4.3 MobileNetV2

MobileNet-v2 is a convolutional neural network that is 53 layers deep. In this research work, the main layers that have been used are one input layer, one conv2d layer, one global average pooling layer, two batch normalization layers, two dropouts layer, and two dense layer. Input layer trained zero parameters and generated the output shape of (none, 64,64,3) which has been also generated by the Conv2d layer by training 84 parameters. MobileNetV2 layer generated multiple output layers which produced and trained 2,257,984 parameters. Global average pooling 2d, Batch normalization and dropout trained 0, 5120,and 0 parameters as well as generated 1280 units. The first dropout layer was added to the dense layer with 256 units and trained 327,936 parameters. At the end, the layers such as batch normalization and dropout had 256 units and trained 1024 parameters followed by the dense layer with 4 units and trained 1028 parameters. Total number of parameters generated were 2,593,176 and trainable parameters were 2,555,992 and 37,184 were non trainable parameters. The architecture of MobileNetV2 is shown in Fig. 9.

3.4.4 ResNet152V2

ResNet152V2 is the extension version of ResNetV1 with 152 layers. In this research, this model has generated multiple output layers which trained 58,331,648 parameters. The layered architecture of the model begins with the input layer, which generates the dynamic batch size with 64×64 height and width along with three channels, i.e., RGB. Later in the convolutional layer, conv2d trained 84 parameters by

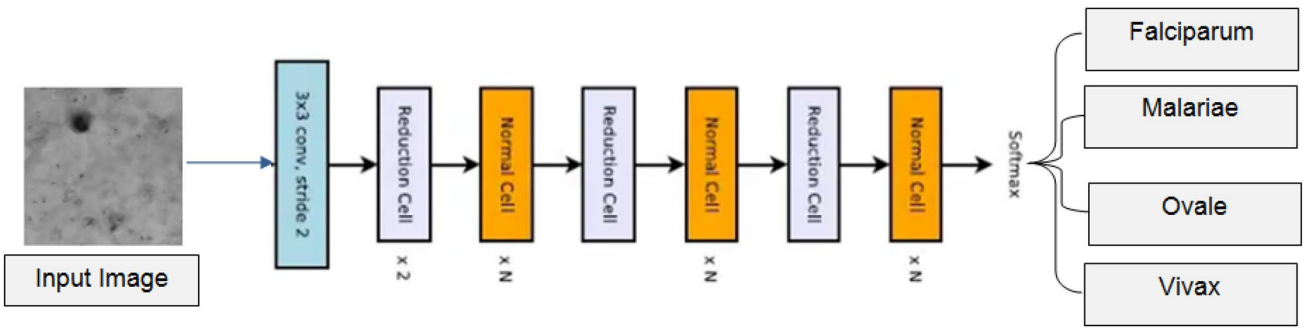

Fig. 8 Architecture of NASNetLarge

generating the output layer of (None, 64,64,3) shape. In the pooling layer, the global average pooling2d layer generated the output shape of 2048 units by training zero parameters. The batch normalization layer generated the output shape of (None, 2048) with 8192 parameters trained by each layer. The dropout layer trained zero parameters, while as dense layer trained 524,544. Batch normalization generated 256 units and trained 1024 parameters. In the end, the dropout layer is added with 256 units trained 0 parameters followed by a dense layer having four and trained 1028 parameters. The total parameters trained by the model are 58,866,520, out of which the trainable parameters are 58,718,168 and the non-trainable parameters are 148,352. The architecture of ResNet152V2 is shown in Fig. 10.

3.4.5 DenseNet121

DenseNet-121 has 120 Convolutions and 4 AvgPool. In this research, an input layer has been used, which trained zero parameters, conv2d trained 84 parameters and generated a dynamic batch size with 64 × 64 height and width and three channels. Densenet121 model developed multiple output layers which trained 7,037,504 parameters. Batch normalization yielded 1024 units and trained 4096 parameters, while as dense layer generated 256 units and trained 262,400 parameters. Likewise, the batch normalization layer, dropout, and dense layer trained 1024, 0, and 1028 parameters, respectively. The total number of parameters generated was 7,306,136, of which 7,219,928 were trainable, and 86,208 were non-trainable. Figure 11 shows the architecture of DenseNet121 used for malaria detection model.

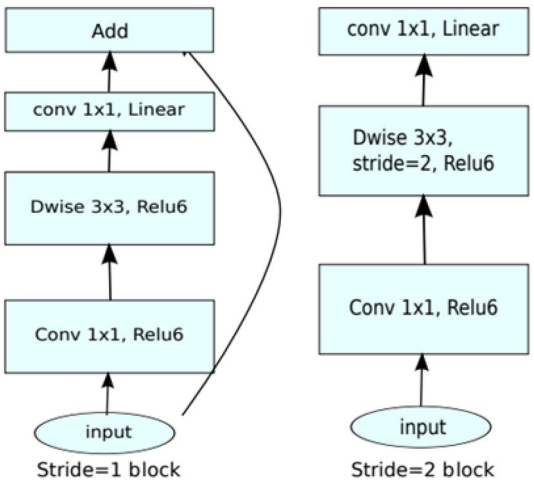

Fig. 9 Architecture of MobileNetV2

3.4.6 Hybrid Model (ResNet152V2 + DenseNet201)

Besides the extended version of the convolutional neural network, we have also hybridized two models, i.e., ResNet152V2 and DenseNet201. The models that worked well for the said dataset were merged to evaluate and compare their performance with the other applied models. In this hybrid structure of the model, layers of the ResNet152V2 model train 58,331,648 parameters, and the layers of the Densenet201 model train 18,321,984 parameters. As per the structure, one input layer has taken the size 64,64,3 and is further connected to the convolution 2d layer, two global average pooling 2d layers, four batch normalization layers, four dropout layers, two dense layers, and one dense layer. In addition, the number of parameters that these layers had trained is shown in Table 2.

3.5 Evaluative Metrics

The models are assessed using a variety of performance metrics, including loss, accuracy, F1 score, recall, and precision, after being trained using the three malaria datasets combined. The model's accuracy tells us whether it correctly identified the output class of an input image. If the model succeeds in doing so, it has been successfully trained and is accepted for validation. A loss occurs when the model predicts the incorrect output class for an image, which is the exact opposite of what it should do. The worse the model

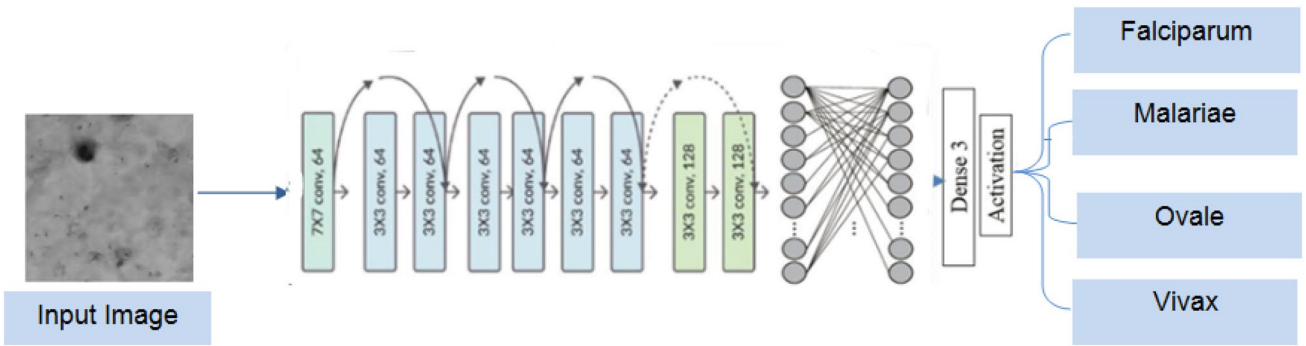

Fig. 10 Architecture of ResNet152V2

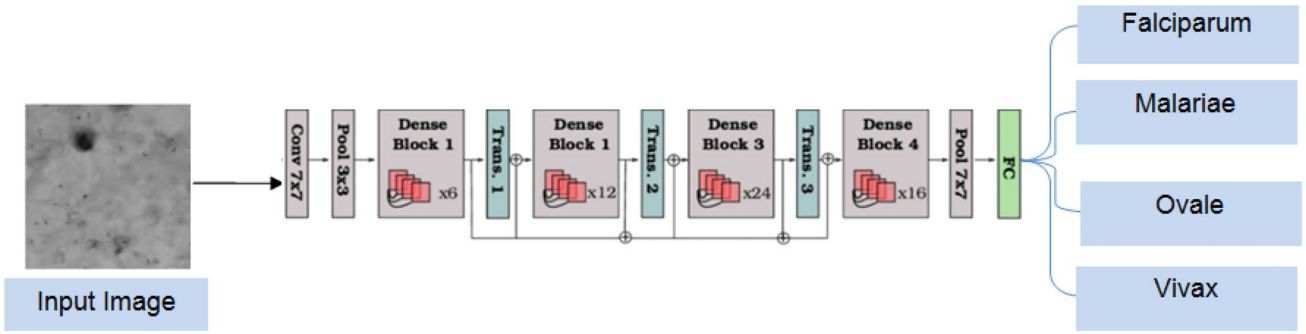

Fig. 11 Architecture of DenseNet121

Table 2 Layered architecture of Hybrid model (DenseNet201 + ResNet152V2)

Layers	Output	Parameters
Input layer	(None, 64,64,3)	0
Conv2D	(None, 64,64,3)	84
ResNet152V2	Multiple	58331648
Global_average_pooling2d	(None,2048)	0
Batch normalization	(None,2048)	8192
Dropout	(None,2048)	0
Dense	(None,256)	524544
Batch normalization	(None,256)	1024
Dropout	(None,256)	0
DenseNet201	Multiple	18321984
Global_average_pooling2d	(None,1920)	0
Batchnormalization	(None,1920)	7680
Dropout	(None,1920)	0
Dense	(None,256)	491776
Batchnormalization	(None,256)	1024
Dropout	(None,256)	0
Dense	(None,4)	1028

performs, the higher the loss value. The equations (18) and (19) are used to calculate these terms [33].

$$Accuracy = \frac{True\ Positive + True\ Negative}{True\ Positive + True\ Negative + False\ Positive + False\ Negative} \quad (18)$$

$$Loss = \frac{(Actual\ Value - Predicted\ Value)^2}{Number\ of\ observations} \quad (19)$$

Precision and recall are the most important metrics for assessing a model's performance. The ratio of relevant instances from the retrieved instances is called precision. It is also known as positive predictive value. In contrast, the proportion of relevant instances which are retrieved is called recall. It is also known as sensitivity. As a result, relevance is necessary for precision and recall. In contrast, the F1 score combines the harmonic mean of a classifier's precision and recall into a single metric. It is primarily used to assess how well two classifiers perform. They can be calculated using the Eqs. (20, 21, and 22) [34].

$$Precision = \frac{True\ Positive}{True\ Positive + False\ Positive} \quad (20)$$

$$Recall = \frac{True\ positive}{True\ positive + False\ Negative} \quad (21)$$

$$F1\ score = 2\frac{Precision * Recall}{Recall + Precision} \quad (22)$$

4 Results and Analysis

In this section, the deep learning models such as DenseNet121, DenseNet201, NasNetLarge, MobileNetV2, ResNet152V2, and hybrid (ResNet152V2 and DenseNet201) that have been applied and trained by the malaria parasite dataset are evaluated using the performance metrics such as accuracy, precision, loss, F1 score, and recall. All the performance has been examined, and their results have been computed during both the training and validation phases. This section also covers the confusion metrics of models for various classes like Falciparum, Ovale, Malariae, and Vivax based on which the performance metrics of the models have been computed.

The highest accuracy and the lowest loss of a model indicate that it is performing well on the given task. Hence, from Table 3, the highest accuracy during a training phase was obtained by the NASNetlarge model and Hybridized model of Resnet152V2 and DenseNet201 with 99.9%. On the contrary, in terms of loss, the best value has been obtained by DenseNet121 with 0.001. The least accuracy and loss value during the same phase has been computed by Resnet152V2

Table 3 Performance of models during training and validation phase of malaria disease detection

Models	Training		Validation	
	Accuracy (%)	Loss	Accuracy (%)	Loss
DenseNet201	99.8	5.58	99.7	1.14
NASNetLarge	99.9	0.05	99.8	1.07
MobileNetV2	98.9	0.02	99.9	1.00
ResNet152V2	99.5	0.02	99.75	0.05
DenseNet121	99.8	0.01	96.50	5.82
Hybrid(ResNet152V2 + DenseNet201)	99.9	0.01	99.8	0.05

Table 4 Examining the models for malaria parasite dataset

Models	Precision	Recall	F1score
DenseNet121	1	1	1
DenseNet201	0.98	0.99	0.9
NASNetLarge	1	1	0.98
MobileNetV2	1	1	0.98
ResNet152V2	1	0.99	1
Hybrid (ResNet152V2 and DenseNet201)	0.99	1	1

with 99.5% and DeneNet201 with 5.58, respectively. Similarly, when the models were evaluated during the validation phase, it was found that MobileNetV2 computed the highest accuracy, and ResNet152V2 had the best loss value of 0.005. The least accuracy and loss value has been calculated by DenseNet121 with 96.50% and 5.82, respectively.

Overall, we can see that all models achieved high accuracy values on the training dataset, but their performance varied on the validation dataset. The hybrid model of ResNet152V2 and DenseNet201 achieved the highest overall performance on both datasets, followed closely by NASNetLarge and MobileNetV2. It is worth noting that DenseNet121 achieved a high accuracy on the training dataset but did not generalize well to the validation dataset, which suggests that the model might be overfitting the training data.

Besides accuracy and loss, the models have also been evaluated for F1 score, precision, and recall score for the complete dataset, as shown in Table 4. DenseNet121 achieved a perfect score of 1 for precision, recall, and F1 score, indicating that it predicted all true positives correctly without any false positives or false negatives. DenseNet201 achieved a high precision of 0.98, recall of 0.99, and F1 score of 0.9. This suggests that while the model performed well in identifying true positives, it might have some false positives or false negatives. NASNetLarge achieved a perfect score of 1 for precision and recall, but a slightly lower F1 score of 0.98. This suggests that the model performed well in identifying true positives and true negatives, but might have some false positives or false negatives. MobileNetV2 achieved a perfect score of 1 for precision and recall, but a slightly lower F1 score of 0.98. This suggests that the model performed well in identifying true positives and true negatives, but might have some false positives or false negatives. ResNet152V2 achieved a perfect score of 1 for precision and F1 score, but a slightly lower recall of 0.99. This suggests that the model performed well in identifying true positives and true negatives, but might have missed some true positives. The hybrid model of ResNet152V2 and DenseNet201 achieved a precision of 0.99, recall of 1, and F1 score of 1, indicating that it performed well in identifying both true positives and true negatives, with few false positives or false negatives.

Overall, we can see that all models achieved high precision, recall, and F1 score values, indicating good performance in identifying true positives and true negatives. The hybrid model of ResNet152V2 and DenseNet201 achieved the highest F1 score, indicating the best overall performance, followed closely by DenseNet121 and ResNet152V2. The same has been shown in terms of the bar graph in Fig. 12.

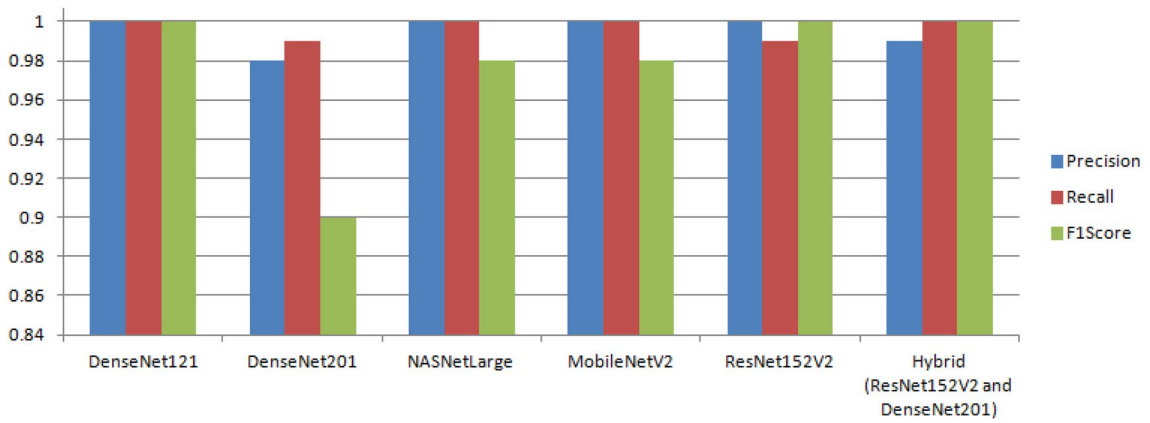

Fig. 12 Analysis of model for other parameters

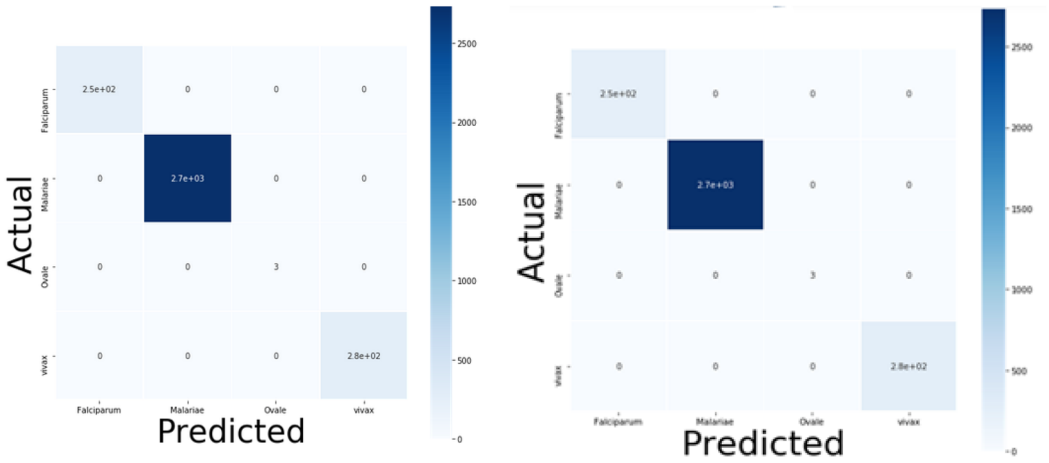

(a) DenseNet201 (b) NASNetLarge

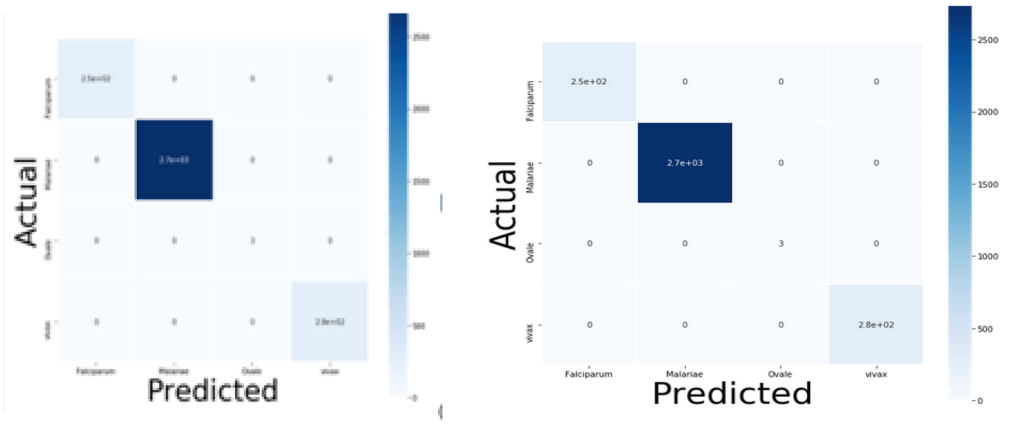

(c)MobileNetV2 (d) ResNet152V2

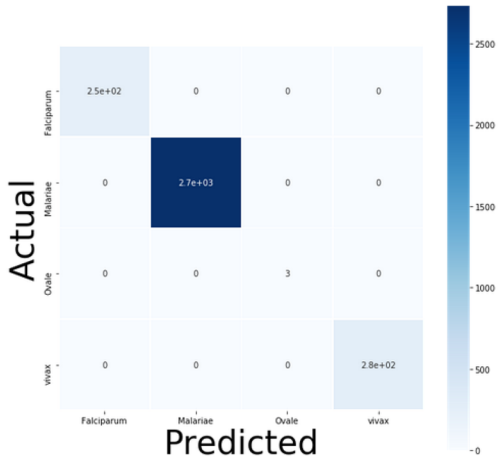

(e) DesneNet121

Fig. 13 Confusion matrix of models for different classes of malaria parasite

Table 5 Performance of models for different classes of malaria parasite dataset

Models	Class	Training		Validation	
		Accuracy (%)	Loss	Accuracy (%)	Loss
DenseNet201	Falciparum	99.59	4.59	99.23	5.34
NASNetLarge		99.41	0.46	99.91	0.59
MobileNetV2		98.46	0.54	98.59	0.59
ResNet152V2		99.59	0.05	99.00	0.26
DenseNet121		99.13	0.05	99.00	0.46
Hybrid(ResNet152V2 + DenseNet201)		99.46	0.02	99.73	0.23
DenseNet201	Malariae	99.49	5.55	99.59	5.59
NASNetLarge		99.46	0.64	99.46	0.06
MobileNetV2		98.75	0.56	98.24	0.06
ResNet152V2		99.23	0.01	99.59	0.04
DenseNet121		99.59	0.06	99.76	0.05
Hybrid(ResNet152V2 + DenseNet201)		99.26	0.08	99.59	0.46
DenseNet201	Ovale	98.45	6.55	99.43	4.59
NASNetLarge		98.44	0.65	99.5	0.60
MobileNetV2		97.76	0.46	98.6	0.50
ResNet152V2		98.24	0.48	99.1	0.05
DenseNet121		98.56	0.15	99.76	0.04
Hybrid(ResNet152V2 + DenseNet201)		98.29	0.20	99.20	0.03
DenseNet201	Vivax	99.59	5.59	99.46	5.59
NASNetLarge		99.3	0.66	99.29	0.65
MobileNetV2		98.7	0.59	98.46	0.54
ResNet152V2		99.6	0.09	99.59	0.05
DenseNet121		99.7	0.02	99.23	0.04
Hybrid(ResNet152V2 + DenseNet201)		99.0	0.02	99.76	0.03

As shown in Fig. 13, the confusion matrix has also been obtained for the applied models to compute the actual and predicted values of the classes such as Falciparum, Malariae, Ovale, and Vivax. We know that a confusion matrix is a table that summarizes the performance of a classification model by comparing its predicted results with the actual results. Moreover, the values in the confusion matrix can be used to calculate various performance metrics, such as accuracy, precision, recall, and F1 score, which can help evaluate the effectiveness of the deep learning model.

In this paper, the 4×4 confusion matrix has been used which includes four categories of predicted labels and four categories of actual labels. Each row in the matrix represents the actual labels, while each column represents the predicted labels. The table lists the counts of observations that belong to each of the four possible combinations of predicted and actual labels. In the confusion matrix of 4×4, the diagonal values represent the true positive values of the respective class and we can compute false positive, false negative, and true negative values from the rest of the rows.

As shown in Table 5, for the Falciparum class, the highest accuracy has been obtained by densenet201, and the hybrid model has computed resnet152v2 with 99.59% and the best loss value with 0.02 during a training phase. Likewise, during the validation phase, the hybrid model obtained the highest accuracy with 99.23% and the best loss value of 0.23. On the contrary, the worst loss value has been obtained by DenseNet201 with 5.34, which is very highest among all loss values. For class Malariae, during the training phase, densenet121 computed the highest accuracy by 99.59%, and ResNet152V2 obtained the best loss value of 0.012. The least has been obtained by DenseNet201 with a 5.55 loss value. Likewise, during the validation phase, the DenseNet121 model computed the highest accuracy, and ResNet152V2 had the best loss value with 99.76% and 0.04, respectively. Here also DenseNet201 showed the least performance in terms of loss value by 5.592. For class Ovale, the highest accuracy of 99.59% and loss value of 0.15 has been obtained by DenseNet121, while DenseNet201 has obtained a bad loss value of 6.56 during the training phase.

On the other hand, for the validation phase, DenseNet121 again embarked the highest value by obtaining an accuracy of 99.76%, and the hybrid model obtained the best loss value of 0.0033. DenseNet201 has obtained the least loss value, on the contrary, with 4.59. For class Vivax, DenseNet121 obtained the highest accuracy with 99.7% and the best loss value with 0.002 at the time of training phase.

Similarly, during the validation phase, the hybrid model computed the highest accuracy of 99.76% and the best loss

Table 6 Analysing models for different classes of malaria parasite dataset

Models	Class	Precision	Recall	F1 score
DenseNet201	Falciparum	0.93	1	0.97
NASNetLarge		0.98	1	0.99
MobileNetV2		1	1	1
ResNet152V2		0.99	0.98	0.99
DenseNet121		0.98	0.99	0.99
Hybrid(ResNet152V2 + DenseNet201)		0.99	0.99	0.99
DenseNet201	Malariae	0.99	0.97	0.98
NASNetLarge		0.99	0.97	0.98
MobileNetV2		0.95	1	0.98
ResNet152V2		0.99	0.95	0.97
DenseNet121		1	1	1
Hybrid(ResNet152V2 + DenseNet201)		1	1	1
DenseNet201	Ovale	1	0.93	0.96
NASNetLarge		1	0.97	0.99
MobileNetV2		1	1	1
ResNet152V2		0.99	0.99	0.99
DenseNet121		1	1	1
Hybrid(ResNet152V2 + DenseNet201)		0.99	0.99	0.99
DenseNet201	Vivax	0.99	1	0.99
NASNetLarge		0.99	1	0.99
MobileNetV2		0.98	1	0.99
ResNet152V2		0.91	1	0.95
DenseNet121		0.99	0.99	0.99
Hybrid(ResNet152V2 + DenseNet201)		0.98	0.98	0.98

value of 0.003. DenseNet201 has again obtained the least loss value with 5.59. On assaying the table overall, it has been found that the DenseNet201 model has not worked well for the models, especially for loss parameters during both the training and validation phases. This is why it has been hybridized with the convenient model to enhance its performance.

Likewise, the models have also been evaluated and examined for different classes of datasets, i.e., Falciparum, Malariae, Ovale, and Vivax using recall, precision, and F1 score in Table 6. During computation, it has been found that for Falciparum, the highest recall, precision, and F1 score value has been obtained by MobileNetV2 while the least precision and DenseNet201 obtained an F1 score with 0.93 and 0.97, respectively, and recall has computed by ResNet152V2 with 0.98. Likewise, for Malariae, DenseNet121 and hybrid model (ResNet152V2 and DenseNet201) calculated the highest precision, F1 score, and recall values. On the contrary, the least precision value for this class has been obtained by MobileNetV2 by 0.95, and recall and F1 score has been acquired by ResNet152V2 with 0.95 and 0.97, respectively. For the Ovale class, the highest values of recall, precision, and F1 score have been achieved by DenseNet121 and MobileNetV2.

On the contrary, for Vivax class, the highest values are taken up by DenseNet201, NASNetLarge, and ResNet152V2 for precision, all the models except DenseNet121 for recall, and in the end, except ResNet152V2 all the models computed the highest F1 score. For Ovale, the least precision, recall, and F1 score have been obtained by ResNet152V2 with 0.99 precision, DensNet201 with 0.93 recall, and 0.96 F1 score. Similarly, for Vivax, the lowest scores are computed by ResNet152V2 in terms of precision and F1 score, while the low recall value is obtained by DenseNet121. The variations of the values achieved by the models for different classes have also been depicted graphically in Fig. 14 through a bar plot.

5 Discussion

CNN is one of the most popular and demanding tools in deep learning, which has shown great and massive success in the medical field. This network has so many hidden layers in the form of a convolution layer, pooling layer, and fully connected layer. All these layers are connected, which helps to learn spatial information from images. The convolutional neural network has been designed for robustly learning massive data of 2d images [35]. Now, as far as this work is concerned, detecting malaria using AI techniques is very helpful for physicians,

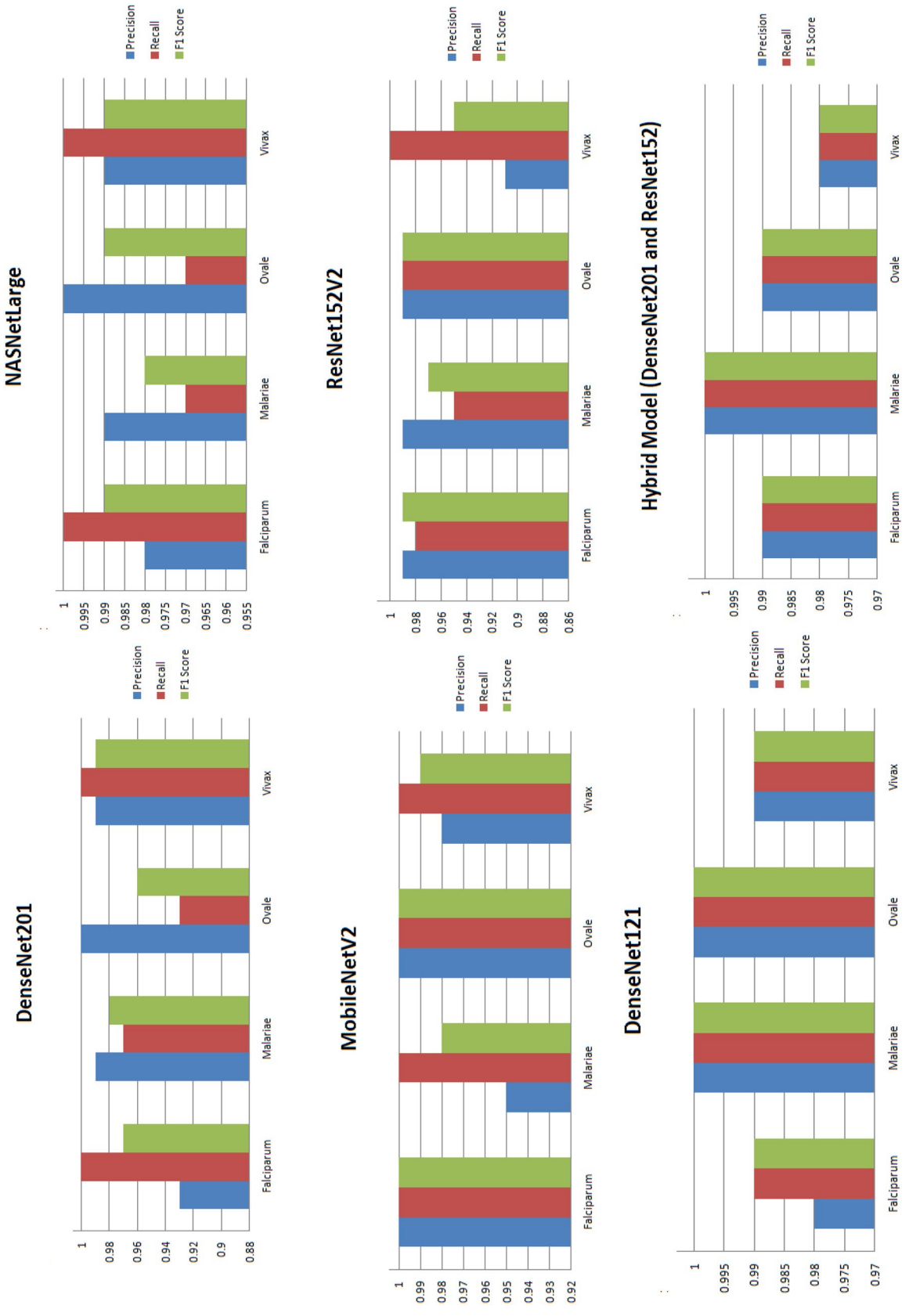

Fig. 14 Performances of models for different classes of malaria parasite

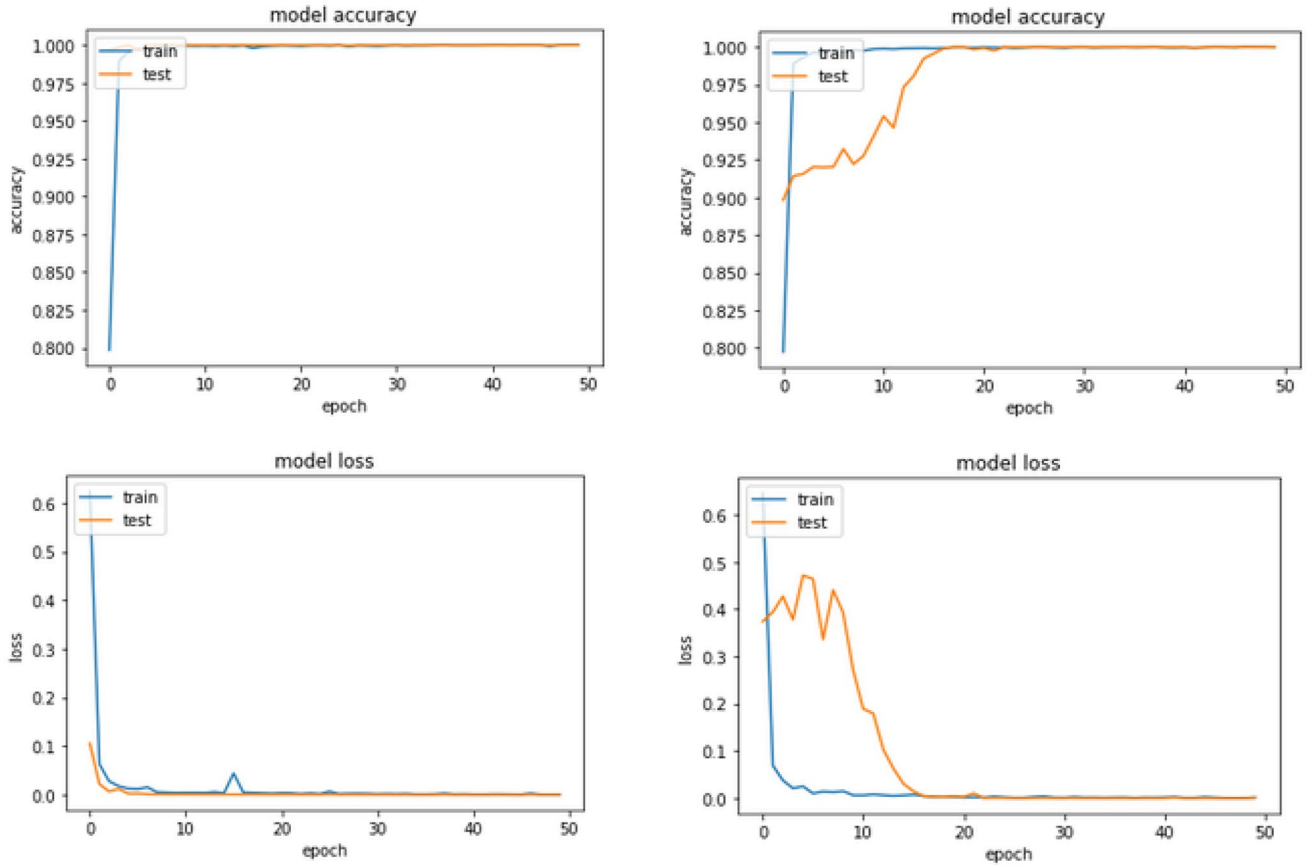

Fig. 15 Graphical analysis of models for detection of malaria disease

lab technicians, radiologists, doctors, etc., as these techniques aid in providing the highest accuracy as well as consistency to diagnose and focus on the part of the images which have pathogens [36]. Traditionally various tests such as rapid diagnostic tests and conventional microscopy are being conducted, which are inclined towards human error. Lack of specificity details and accuracy entirely rely on human judgment, which is usually biased [37–41]. Hence, there is a compulsory need to benchmark AI-based techniques for identifying and classifying malaria parasites. In this paper, we have developed a model for the detection and classification of malaria parasites in microscopic images to save people from major illnesses using deep learning techniques. We have used the images from three different sources of malaria parasites to generate four classes such as Falciparum, Malariae, Ovale, and Vivax, and trained them on various deep learning models, such as a DenseNet201, DenseNet121, NASNet Large, MobileNetV2, ResNet152V2 and a hybrid model of ResNet152V2 and DenseNet201. The models were trained for 50 epochs, and their performances were evaluated initially using accuracy and loss. The results have been computed and discussed in Sect. 4. Besides this, their graphs were also generated in Fig. 15 and analyzed for different epochs.

From the training and validation curves, we can easily and clearly state that all the models have shown a good fit for learning. At a few epochs, certain peaks have been formed, such as in NASNetLarge, Hybrid model, but overall they have also shown a good fit of learning for both accuracy and loss curves. It indicates that the algorithm's learning lies in between an underfit and overfit of the model, which means that the validation and training accuracy, as well as loss, decreases to a certain point of stability with a very minimal gap. In addition to this, the time frame taken by the models to get trained by the images of 4 classes has also been computed such as Densenet121 took 1hr50min, NASNetLarge took 5 h, DenseNet201 took 16hrs20min, mobileNetV2 took 3hrs60min, Resnet152v2 took 10hrs46min59sec, and at the end the hybridization of DenseNet201 and ResNet152v2 took 20hr1min53sec. On assaying the time, it has been found that less time has been taken for DenseNet121 with 1 h 50 min compared to other algorithms. On the contrary, the maximum time has been consumed by the hybridization of ResNet152V2 and DenseNet201 by 20hrs1min53sec. Besides this, the performance of the models for this research work has been compared with few of the existing techniques, as shown in Table 7.

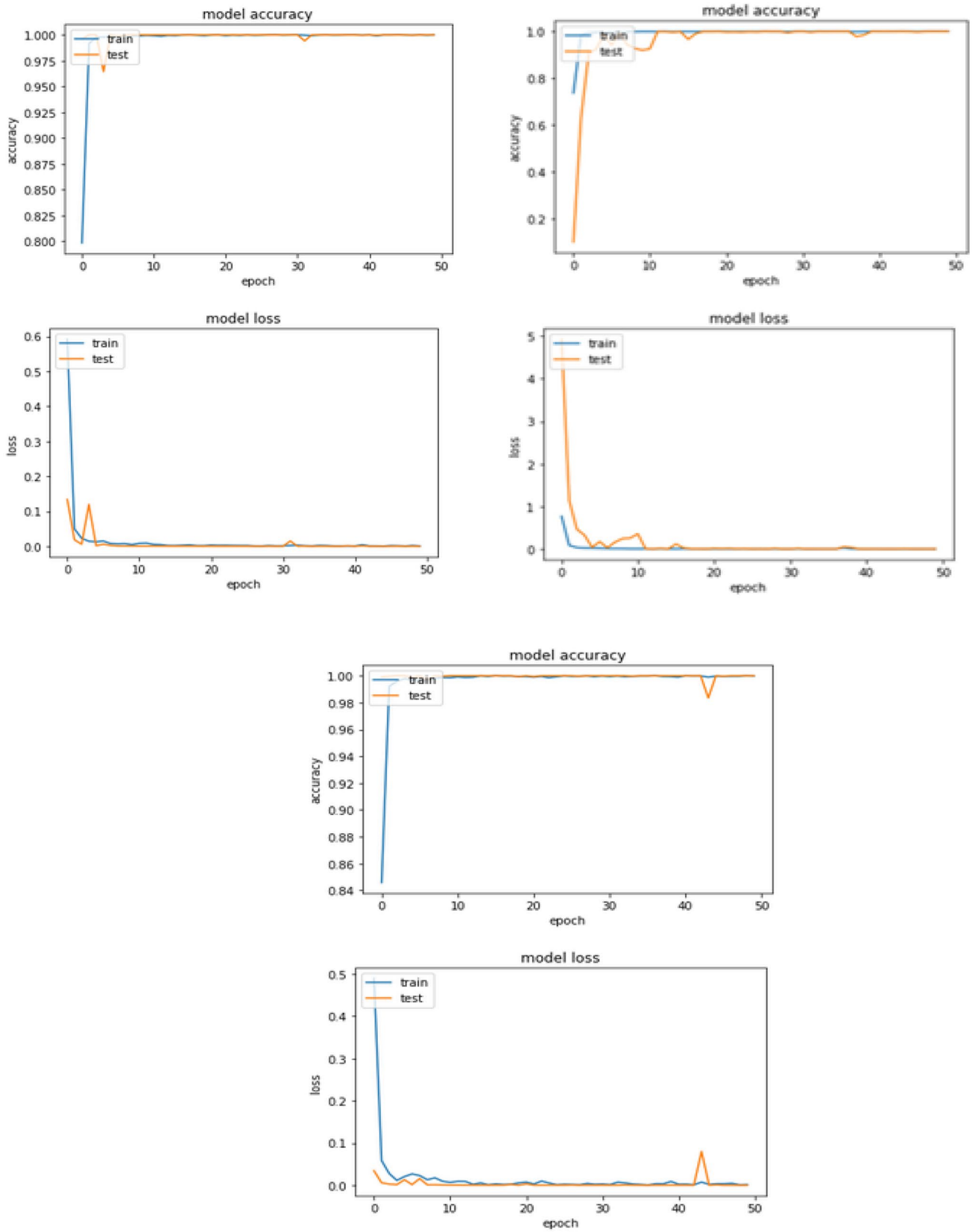

Fig. 15 (continued)

Table 7 Comparison with the state-of-the-art

References	Dataset	Technique	Accuracy (%)
[16]	27,558 cell images	CNN + SVM	96.7
[18]	Images of falciparum malaria parasite	VGG + SVM	93.1
[20]	Data collected from 2014 to 2018	XGB Classifier	90.97
[26]	27,558 images	Naïve Bayes	84
Our study	Images of Falciparum, Vivax, Ovale, and Malariae	MobileNetV2	99.9

6 Conclusion

Malaria is one of the severe health issues around the globe that has killed millions of people every year. Doctors have tried their best to diagnose it using light microscopy, but it requires well-trained and experienced microscopists. Hence, in artificial intelligence, new techniques to analyze digital medical images are a challenging tool to diagnose such infectious diseases. Mostly, AI-based techniques such as convolutional neural networks emulate the microscopy visualization of an expert to detect the image of malaria parasites at a meagre cost and fast diagnosis, and that too under less supervision. In this paper, we have taken four classes of malaria parasite datasets and applied them to advanced deep-learning techniques. The models were evaluated based on various performance metrics where it was found that DenseNet121 obtained the highest accuracy of 99.9% compared to the other models. Before feeding the models, the images were pre-processed, and features were extracted from them as highlighted regions. The main limitation encountered during the research was the high computational time taken by the models during the training period though they provided better results. In addition, the work was performed on a limited training dataset, which resulted in an overfitting modelling error, and was also observed in the performance of the applied models. Hence, in the future, the developed model could be used by research fraternities to extend the classification of other malaria parasites. In addition, the layers of the deep learning models should also be hyper-tuned so that they will take a minimal amount of time to get processed and display the result as fast as possible. Besides this, more images should also be incorporated to train the model for better detection and classification of the malaria parasite. In a nut shell, the deep learning models should be used to reduce the burden on healthcare professionals and make malaria diagnosis more accessible to people in remote areas. Infact, deep learning models developed for malaria detection could potentially be adapted to diagnose other diseases as well, such as dengue fever or Zika virus.

Funding Not applicable.

Data Availability Not applicable.

Code Availability Not applicable.

Declarations

Conflict of interest The authors declare that they have no conflict of interest.

References

1. Gourisaria MK, Das S, Sharma R, Rautaray SS, Pandey M (2020) A deep learning model for malaria disease detection and analysis using deep convolutional neural networks. Int J Emerg Technol 11(2):699–704
2. Tuteja R (2007) Malaria– an overview. FEBS J 274(18):4670–4679
3. Fried M, Duffy PE (2017) Malaria during pregnancy. Cold Spring Harb Perspect Med 7(6):a025551
4. World Health Organization (2022) World malaria report 2022. World Health Organization, Geneva
5. Uneke CJ, Duhlinska DD, Ujam TN (2009) Effects of maternal plasmodium falciparum malaria and HIV infection on birth weight in southeastern Nigeria. McGill J Med: MJM 12(2):49
6. Yang D, Subramanian G, Duan J, Gao S, Bai L, Chandramohanadas R, Ai Y (2017) A portable image-based cytometer for rapid malaria detection and quantification. PLoS ONE 12(6):e0179161
7. Hakizimana D, Ntizimira C, Mbituyumuremyi A, Hakizimana E, Mahmoud H, Birindabagabo P, Gashumba D (2022) The impact of Covid-19 on malaria services in three high endemic districts in Rwanda: a mixed-method study. Malar J 21(1):1–17
8. World Health Organization (2016) World malaria report 2015. World Health Organization, Geneva
9. Sharma S, Verma R, Yadav B, Kumar A, Rahi M, Sharma A (2022) What India can learn from globally successful malaria elimination programmes. BMJ Glob Health 7(6):e008431
10. Mbanefo A, Kumar N (2020) Evaluation of malaria diagnostic methods as a key for successful control and elimination programs. Trop Med Infect Dis 5(2):102
11. Nema S, Rahi M, Sharma A, Bharti PK (2022) Strengthening malaria microscopy using artificial intelligence-based approaches in India. Lancet Reg Health-Southeast Asia 5:100054
12. Daid R, Kumar Y, Gupta A, Kaur I (2021, November) An effective mechanism for early chronic illness detection using multilayer convolution deep learning predictive modelling. In 2021 international conference on technological advancements and innovations (ICTAI), IEEE. pp. 649–652
13. Bansal K, Bathla RK, Kumar Y (2022) Deep transfer learning techniques with hybrid optimization in early prediction and diagnosis of different types of oral cancer. Soft Comput 26(21):11153–11184

14. Beck HP (2022) Digital microscopy and artificial intelligence could profoundly contribute to malaria diagnosis in elimination settings. Front Artif Intell 5:510483
15. Kumar Y, Koul A, Mahajan S (2022) A deep learning approaches and fastai text classification to predict 25 medical diseases from medical speech utterances, transcription and intent. Soft Comput 26(17):8253–8272
16. Narayanan BN, Ali R, Hardie RC (2019) Performance analysis of machine learning and deep learning architectures for malaria detection on cell images. In: Zelinski ME, Taha TM, Howe J, Awwal AAS, Iftekharuddin KM (eds) Applications of machine learning. SPIE, Bellingham, pp 240–247
17. Shekar G, Revathy S, Goud EK (2020, June) Malaria detection using deep learning. In 2020 4th international conference on trends in electronics and informatics (ICOEI)(48184), IEEE. pp. 746–750
18. Vijayalakshmi A (2020) Deep learning approach to detect malaria from microscopic images. Multimed Tools Appl 79(21):15297–15317
19. Bhuiyan M, Islam MS (2023) A new ensemble learning approach to detect malaria from microscopic red blood cell images. Sens Int 4:100209
20. Ruban S, Naresh A, Rai S (2023) An ensemble approach for detecting malaria using classification algorithms. In: Shetty NR, Patnaik LM, Prasad NH (eds) Emerging research in computing, information, communication and applications. Springer, Singapore, pp 307–315
21. Alnussairi MHD, İbrahim AA (2022) Malaria parasite detection using deep learning algorithms based on (CNNs) technique. Comput Electr Eng 103:108316
22. Masud M, Alhumyani H, Alshamrani SS, Cheikhrouhou O, Ibrahim S, Muhammad G, Shorfuzzaman M (2020) Leveraging deep learning techniques for malaria parasite detection using mobile application. Wirel Commun Mobile Comput. https://doi.org/10.1155/2020/8895429
23. Dong Y, Jiang Z, Shen H, Pan WD, Williams LA, Reddy VV, Bryan AW (2017, February) Evaluations of deep convolutional neural networks for automatic identification of malaria infected cells. In 2017 IEEE EMBS international conference on biomedical & health informatics (BHI), IEEE. pp. 101–104
24. Nayak S, Kumar S, Jangid M (2019, September) Malaria detection using multiple deep learning approaches. In 2019 2nd International Conference on Intelligent Communication and Computational Techniques (ICCT), IEEE. pp. 292–297
25. Pattanaik PA, Mittal M, Khan MZ (2020) Unsupervised deep learning cad scheme for the detection of malaria in blood smear microscopic images. IEEE Access 8:94936–94946
26. Soomro A, Baloch ERB, Jawaid MM, Zehra Q, Babar N (2021) Malaria cells image analysis using image processing filters and naïve bayes classifier. Eng Sci Technol Int Res J 5(1):18–23
27. Jha KK, Dutta HS (2019) Mutual information based hybrid model and deep learning for acute lymphocytic leukemia detection in single cell blood smear images. Comput Methods Progr Biomed 179:104987
28. Dĩker, A. (2022) An efficient model of residual based convolutional neural network with Bayesian optimization for the classification of malarial cell images. Comput Biol Med 148:105635
29. Mohamed EH, El-Behaidy WH, Khoriba G, Li J (2020) Improved white blood cells classification based on pre-trained deep learning models. J Commun Softw Syst 16(1):37–45
30. Loddo A, Di Ruberto C, Kocher M, Prod'Hom G (2018) MP-IDB: the malaria parasite image database for image processing and analysis. In: Lepore N, Brieva J, Romero E, Racoceanu D, Joskowicz L (eds) Sipaim-miccai biomedical workshop. Springer, Cham, pp 57–65
31. Koul A, Kumar Y, Gupta A (2022, October) A study on bladder cancer detection using AI-based learning techniques. In 2022 2nd International Conference on Technological Advancements in Computational Sciences (ICTACS), IEEE. pp. 600–604
32. Koul A, Bawa RK, Kumar Y (2022) Artificial intelligence techniques to predict the airway disorders illness: a systematic review. Arch Comput Methods Eng 30:1–34
33. Yamashita R, Nishio M, Do RKG, Togashi K (2018) Convolutional neural networks: an overview and application in radiology. Insights Imaging 9(4):611–629
34. Kaur I, Sandhu AK, Kumar Y (2022) Artificial intelligence techniques for predictive modeling of vector-borne diseases and its pathogens: a systematic review. Arch Computat Methods Eng 29:3741–3771. https://doi.org/10.1007/s11831-022-09724-9
35. Fuhad KM, Tuba JF, Sarker M, Ali R, Momen S, Mohammed N, Rahman T (2020) Deep learning based automatic malaria parasite detection from blood smear and its smartphone based application. Diagnostics 10(5):329
36. Kumar A, Kumar N, Kuriakose J et al (2023) A review of deep learning-based approaches for detection and diagnosis of diverse classes of drugs. Arch Computat Methods Eng. https://doi.org/10.1007/s11831-023-09936-7
37. Sisodia PS, Ameta GK, Kumar Y et al (2023) A review of deep transfer learning approaches for class-wise prediction of Alzheimer's disease using MRI images. Arch Computat Methods Eng 30:2409–2429. https://doi.org/10.1007/s11831-022-09870-0
38. Kaur S, Kumar Y, Koul A et al (2023) A systematic review on metaheuristic optimization techniques for feature selections in disease diagnosis: open issues and challenges. Arch Computat Methods Eng 30:1863–1895. https://doi.org/10.1007/s11831-022-09853-1
39. Kaur I, Sandhu AK, Kumar Y. (2022) A hybrid deep transfer learning approach for the detection of vector-borne diseases. 2022 5th International Conference on Contemporary Computing and Informatics (IC3I), Uttar Pradesh, India, 2189–2194.https://doi.org/10.1109/IC3I56241.2022.10072576.
40. Moody A (2002) Rapid diagnostic tests for malaria parasites. Clin Microbiol Rev 15(1):66–78
41. Kumar Y, Koul A, Mahajan S (2022) A deep learning approaches and fastai text classification to predict 25 medical diseases from medical speech utterances, transcription and intent. Soft Comput 26:8253–8272. https://doi.org/10.1007/s00500-022-07261-y
42. https://www.cdc.gov/parasites/malaria/index.html